Am J Transl Res 2024;16(3):755-767
www.ajtr.org /ISSN:1943-8141/AJTR0147047

Original Article

Screening of potential biomarkers in propofol-induced neurotoxicity via bioinformatics prediction and experimental verification

Tianping He[1*], Jianfeng Huang[1*], Bo Peng[1], Mianhui Wang[1], Qiuhao Shui[1], Liang Cai[2]

[1]Department of Anesthesiology, Luxian People's Hospital, Luzhou 646100, Sichuan, China; [2]Department of Anesthesiology, The People's Hospital of Leshan, Leshan 614013, Sichuan, China. [*]Equal contributors.

Received October 16, 2022; Accepted December 16, 2022; Epub March 15, 2024; Published March 30, 2024

Abstract: Objectives: To identify hub genes and biological processes of propofol-induced neurotoxicity and promote the development of pediatric anesthesiology. Methods: We downloaded the GSE106799 dataset from the Gene Expression Omnibus database. Differentially expressed genes (DEGs) were screened, then Kyoto Encyclopedia of Genes and Genomes, Gene Ontology and Gene Set Enrichment analyses were performed on all DEGs. We identified potential ferroptosis genes in the pathogenesis of propofol-induced neurotoxicity. A key module was obtained after performing weighted gene co-expression network analysis (WGCNA) on the GSE106799 dataset. Hub genes were identified after the least absolute shrinkage and selection operator (LASSO) regression analysis of the intersection of DEGs and genes from the key module. We established a competing endogenous RNA network and predicted potential drugs according to the hub genes. Total RNA and proteins were extracted for real-time quantitative polymerase chain reaction and Western blotting, respectively. Results: A total of 112 DEGs, including 76 upregulated and 36 downregulated ones were screened out. Propofol-induced neurotoxicity involved processes such as nervous system development, activation of JAK/STAT and MAPK signaling pathways, vascular regeneration, and oxidative stress. The results of WGCNA suggested that the tan module was the most strongly associated with propofol-induced neurotoxicity. We identified 4 hub genes (*EGR4, HAO1, ITK and GM14446*) after LASSO regression analysis. Animal experiments demonstrated that propofol caused overexpression of the protein levels of *HAO1, ITK* and inflammatory factors in the brain, as well as the mRNA levels of *HAO1, ITK* and *GM14446*. Propofol inhibited expression of *EGR4* at mRNA and protein levels. Conclusions: Previous studies have demonstrated that *EGR4, HAO1, ITK* and *GM14446* play a role in intellectual development, neuroinflammation and neuronal differentiation. These hub genes may help us to find new preventive and therapeutic targets for propofol-induced neurotoxicity.

Keywords: Propofol, neurotoxicity, potential biomarkers

Introduction

In the early 20th century, general anesthesia was not usually adopted in pediatric surgery to prevent hemodynamic depression. At that time, it was generally believed that children could not perceive or locate pain. With the accumulation of clinical experience and the gradual progress of testing, physicians have realized that pain causes a severe stress response in children [1, 2]. With the continuous development of pediatric anesthesiology, ketamine, propofol and other anesthetics have been gradually applied to pediatric surgery in recent years. However, the medical community began to focus on young children with neurological damage due to general anesthesia approximately 10 years ago. Researchers have also found that all conventionally applied sedative anesthetics cause neurotoxicity in animal models [3]. Many studies and individual cases have attributed perioperative neurotoxicity and neurogenic injury to propofol [4, 5]. Neurotoxicity induced by propofol involves different pathological mechanisms including calcium overload, ferroptosis, neuroinflammation and excitotoxicity [6]. The complexity of human brain structure and function may account for the greater vulnerability of the human brain to injury compared with animal brains. The application of bioinformatics makes

https://doi.org/10.62347/MTAY7931

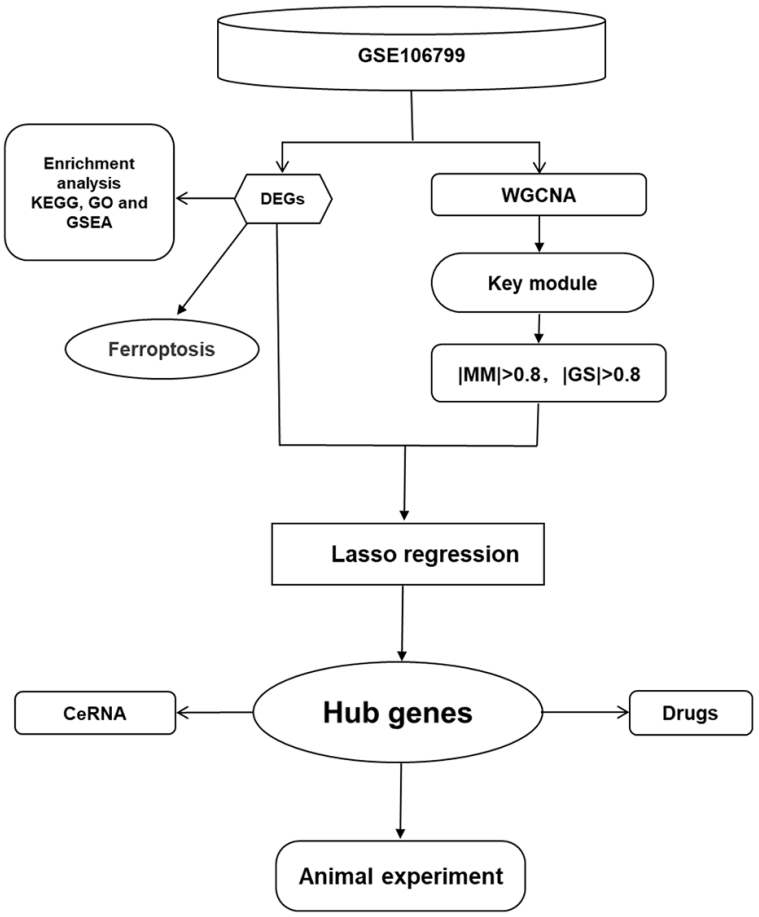

Figure 1. Study workflow.

it convenient to screen for hub genes in propofol-induced neurotoxicity.

Although the concept of anesthetic neurotoxicity was proposed over 10 years ago, the behind mechanism remains unclear. Epidemiological studies have found that general anesthesia may lead to learning disabilities and language disorders in children younger than 4 years old [2, 7]. Propofol is one of the most frequently used anesthetics in clinical practice. Therefore, it is important to explore the specific mechanism of propofol-induced neurotoxicity. Bioinformatics can analyze the mechanism of diseases from different aspects based on its large calculation capability. Firstly, we screened significant differentially expressed genes (DEGs) introduced by propofol in the GSE106799 dataset. Secondly, new research revealed that anesthetic neurotoxicity may involve ferroptosis, so we identified some DEGs associated with ferroptosis in the GSE106799 dataset. Thirdly, we explored the signaling pathway and biological function involved in propofol-induced neurotoxicity through enrichment analysis. Fourthly, we obtained the module with the highest correlation with propofol-induced neurotoxicity via weighted gene co-expression network analysis (WGCNA), and obtained key modular DEGs by intersecting key mo-dular genes and DEGs. Hub genes were obtained after least absolute shrinkage and selection operator (LASSO) regression analysis of key modular DEGs. Fifthly, we built a network of competing endogenous RNA (ceRNA) and drugs according to hub genes that may help us to find potential targets or drugs. Finally, we used animal experiments to identify whether the expression of hub genes was the same as those in previous analyses. Clinical studies about anesthetic neurotoxicity have been scarce. There is no definite diagnosis and treatment outline for propofol-induced neurotoxicity. We hope that our results will help physicians diagnose and treat propofol-induced neurotoxicity.

Materials and methods

Workflow

The workflow of this study is outlined in **Figure 1**.

Data source and materials

The GSE106799 dataset obtained from the Gene Expression Omnibus database (https://www.ncbi.nlm.nih.gov/gds) is a collection of mRNA sequence from brain tissue of mice treated by propofol. This dataset included 4 mice treated with 50 mg/kg propofol as case group and 4 mice treated with 50 mg/kg lipid vehicle as control group. All R Packages were

Table 1. Specific primer sequences for hub genes

GENES	Forward primer	Reverse primer
GM14446	5'-TGGGCCTACTTGGGTTTGTC-3'	5'-ACTCAGGGTTCACTGCTCCT-3'
HAO1	5'-CCTGGATGGGGGAGTAAGGA-3'	5'-GGTCTTCCCACAAAAACGGC-3'
ITK	5'-TGTGTACTTACAGGTCGTGC-3'	5'-ACAAGGCAATGACCAGGGTT-3'
EGR4	5'-CGACTTCTTGAGCTGGGCTT-3'	5'-ATCTGGGGAGTAGAGGTCCG-3'
GAPDH	5'-ATGGGAAGCTGGTCATCAAC-3'	5'-GGATGCAGGGATGATGTTCT-3'

downloaded from The Comprehensive R Archive Network (https://cran.r-project.org). The following antibodies were obtained, anti-EGR4 (ab198197, Abcam), anti-IL-6 (ab259341, Abcam), anti-HAO1 (ab194790, Abcam), anti-NF-κB (ab32536, Abcam) and anti-ITK (PA5-29669, ThermoFisher). RIPA lysis buffer (FD009), protein phosphatase inhibitor (FD1002) and phenylmethanesulfonyl fluoride (FD0100) used for tissue lysis were obtained from FUDE Biotechnology Company. Universal RNA Extraction Kit (No: 9767), PrimeScript™ RT Master Mix (No: 036A) and TB Green Premix Ex Taq II (Tli RNaseH Plus, No. 820A) were purchased from TaKaRa.

Quantitative real-time polymerase chain reaction (qRT-PCR)

Total RNA was extracted from the brain tissue using Universal RNA Extraction Kit. Total RNA was transcribed into cDNA using PrimeScript™ RT Master Mix. cDNA (2 μl) was used for qRT-PCR using TB Green Premix Ex Taq II (Tli RNaseH Plus, No. 820A). The PCR conditions were as follows, pre-denaturation at 95°C for 30 seconds, 40 cycles of 5 seconds at 95°C and 34 seconds at 60°C, and dissociation at 60°C and 95°C. The relative expression of mRNA was calculated by $2^{-\Delta\Delta Ct}$ method with normalization to GAPDH. The primers were synthesized by Tsingke Biotechnology. The primer sequences are shown in **Table 1**.

Western blotting

Total protein was obtained by using buffer composed of 0.5 ml RIPA lysis buffer, 5 μl protein phosphatase inhibitor and 5 μl phenylmethanesulfonyl fluoride. Total protein was denatured in water at 100°C for 5 minutes. The samples were subjected to 90 V electrophoresis for 25 minutes, followed by 120 V until the end. The protein from the gel was transferred to polyvinylidene fluoride membrane at 200 mA for 90 minutes. Membranes were blocked using 5% bovine serum albumin at room temperature. We incubated the membrane in antibody working solution for 12 hours. Fluorescent secondary antibody working solution was applied to display the target protein. Blot images were dealt by ODYSSEY System and Image J software.

Differential expression analysis

To identify DEGs between two groups and to perform in-depth functional mining, the limma package was used to identify genes with $P<0.05$ and $|log2FC| >1$ as DEGs. Over-expressed genes were distinguished from repressed genes by different colors in heatmaps. Finally, we screened the DEGs and mapped volcanoes.

Functional enrichment analysis

To explore the functional genes, proteins and signaling pathways involved in propofol-induced neurotoxicity, the clusterProfiler package in R was used for Gene Ontology (GO) and Kyoto Encyclopedia of Genes and Genomes (KEGG) analyses. In addition, we performed gene set enrichment analysis (GSEA) to observe the distribution of DEGs in different phenotypes.

WGCNA

The co-expression network was constructed by the WGCNA package in R. Firstly, we clustered the samples according to clinical traits. Secondly, we built the co-expression network via the automatic network construction function. The soft thresholding power, to which co-expression similarity was applied to calculate adjacency, was calculated by the R function pick SoftThreshold. Thirdly, hierarchical clustering and the dynamic tree cut function were used to detect modules according to MEDissThres set at 0.25. This research focused on modules associated with propofol-induced neurotoxicity, so we screened modules with the non-gray module, the smallest *P* value and the

highest correlation with propofol-induced neurotoxicity.

Hub genes in propofol-induced neurotoxicity

Genes from the key module were plotted as a scatter plot, and we screened out the key genes of this module with the criteria of gene significance (GS) >0.8 and module membership (MM) >0.8. We identified key modular DEGs by intersecting genes from the key module and the DEGs. Finally, we obtained hub genes of propofol-induced neurotoxicity by LASSO regression analysis of key modular DEGs. Thereafter, receiver operating characteristic (ROC) curves of hub genes were plotted to verify their ability to distinguish control and case samples. Finally, boxplots were used to reveal the expression trends of hub genes.

Ferroptosis-related genes

Previous research has suggested that propofol-induced neurotoxicity involves ferroptosis [8]. We obtained ferroptosis-related genes by taking the intersection of genes related to ferroptosis and the DEGs.

ceRNA network construction and drug prediction

We established an mRNA-miRNA-lncRNA ceRNA network via the miRWalk website (http://mirwalk.umm.uni-heidelberg.de/) and the miRBD database (http://mirdb.org). We predicted potential drugs based on hub genes via the CTD database (http://ctdbase.org/). The results were visualized using cytoscape software.

Animal experiments

C57 mice were obtained from the Laboratory Animal Center of Guangxi Medical University. The license for the application of laboratory animals was SCXK 2014-0003. Mice were randomly divided into case and control groups, with 5 in each group. Mice in the case group were injected intraperitoneally with 50 mg/kg propofol, and mice in the control group were injected intraperitoneally with 50 mg/kg lipid vehicle. Mice were sacrificed, and their brain tissues were rapidly removed 3 hours after intraperitoneal injection of these agents. Western blotting was used to test the protein expression levels of *EGR4, HAO1, ITK,* IL-6 and NF-κB in the brain tissue. The mRNA expression levels of *EGR4, HAO1, ITK* and *GM14446* in the 2 groups were detected by qRT-PCR.

Statistical analyses

All data from the GSE106799 dataset were analyzed by the R package. Data from animal experiments are presented as mean ± standard deviation (SD) and were analyzed by Student's *t* test or Kruskal-Wallis-Test. Statistical analyses were performed using GraphPad Prism 8 and SPSS 22.0. $P<0.05$ was considered statistically significant.

Results

Obtained DEGs and enrichment analysis

We identified 112 significant DEGs consisting of 36 downregulated and 76 upregulated ones (**Figure 2A**). The top 90 DEGs between the control and case groups were exhibited with a heatmap (**Figure 2B**). When we performed KEGG enrichment and GO functional analysis on all DEGs, it was found that propofol-induced neurotoxicity involved 12 functional entries and 4 signaling pathways, such as somite rostral, protein tyrosine, neuroactive ligand-receptor interaction and retinol metabolism (**Figure 2C**, **2D**). GSEA of the DEGs suggested that propofol-induced neurotoxicity was associated with processes such as activation of $CD8^+$ T cells, B cell maturation and transcription of Pam3CSK4 (**Figure 2E**, **2F**).

Construction of gene co-expression modules

To check the overall correlation of all samples in the GSE106799 dataset, we constructed sample clustering and clinical trait heatmaps by clustering data and removing outliers (**Figure 3A**). The results of the analysis suggested that the interaction of genes at an optimal power of 10 maximally fitted the scale-free distribution (**Figure 3B**). A total of 12 modules were clustered in the module cluster dendrogram, and tan module was found to be the most highly associated with propofol-induced neurotoxicity, according to the statistics (**Figure 3C**, **3D**). The tan module contained 68 genes. After screening according to the criteria of |MM| >0.8 and |GS| >0.8, 27 key modular genes were obtained (**Figure 3E**).

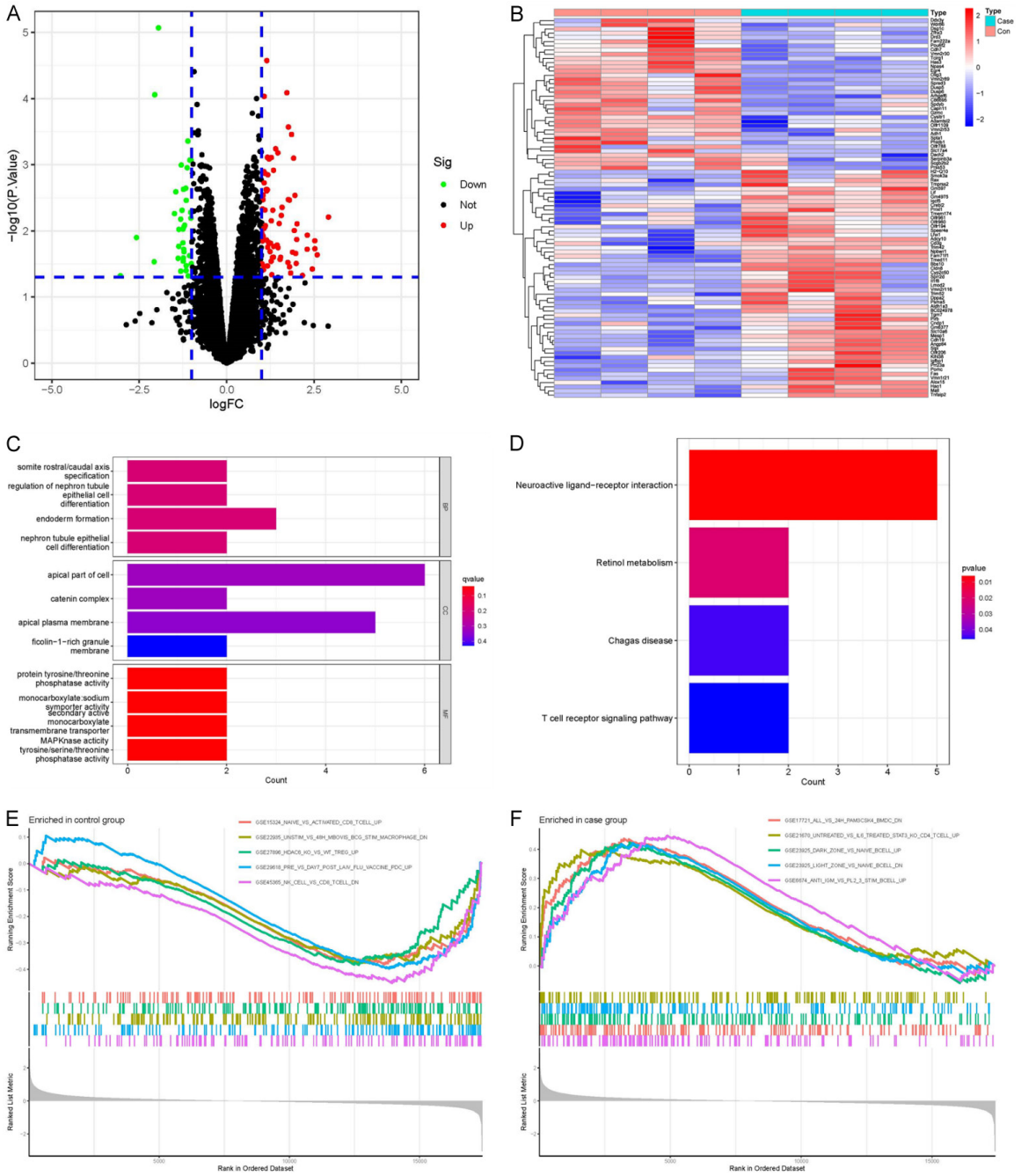

Figure 2. DEGs and enrichment analysis. A. Volcano plot of DEGs. B. Heatmap of DEGs. Red represents high expression, and blue represents low expression. C-F. Enrichment analysis: GO, KEGG and GSEA. DEDs: Differentially Expressed Genes; GO: Gene Ontology; KEGG: Kyoto Encyclopedia of Genes and Genomes; GSEA: Gene Set Enrichment Analysis.

Acquisition of 4 hub genes

The intersection of DEGs and key modular genes resulted in 25 key modular DEGs (**Figure 4A**). These were subjected to LASSO regression analysis and 4 hub genes (*EGR4, HAO1, ITK* and *GM14446*) were screened out (**Figure 4B**, **4C**). The areas under the ROC curves for hub genes were all 1, which indicated that the model performed well (**Figure 4D-G**).

Ferroptosis-related genes

There were 24 DEGs related to ferroptosis in the GSE106799 dataset. See **Figure 5**.

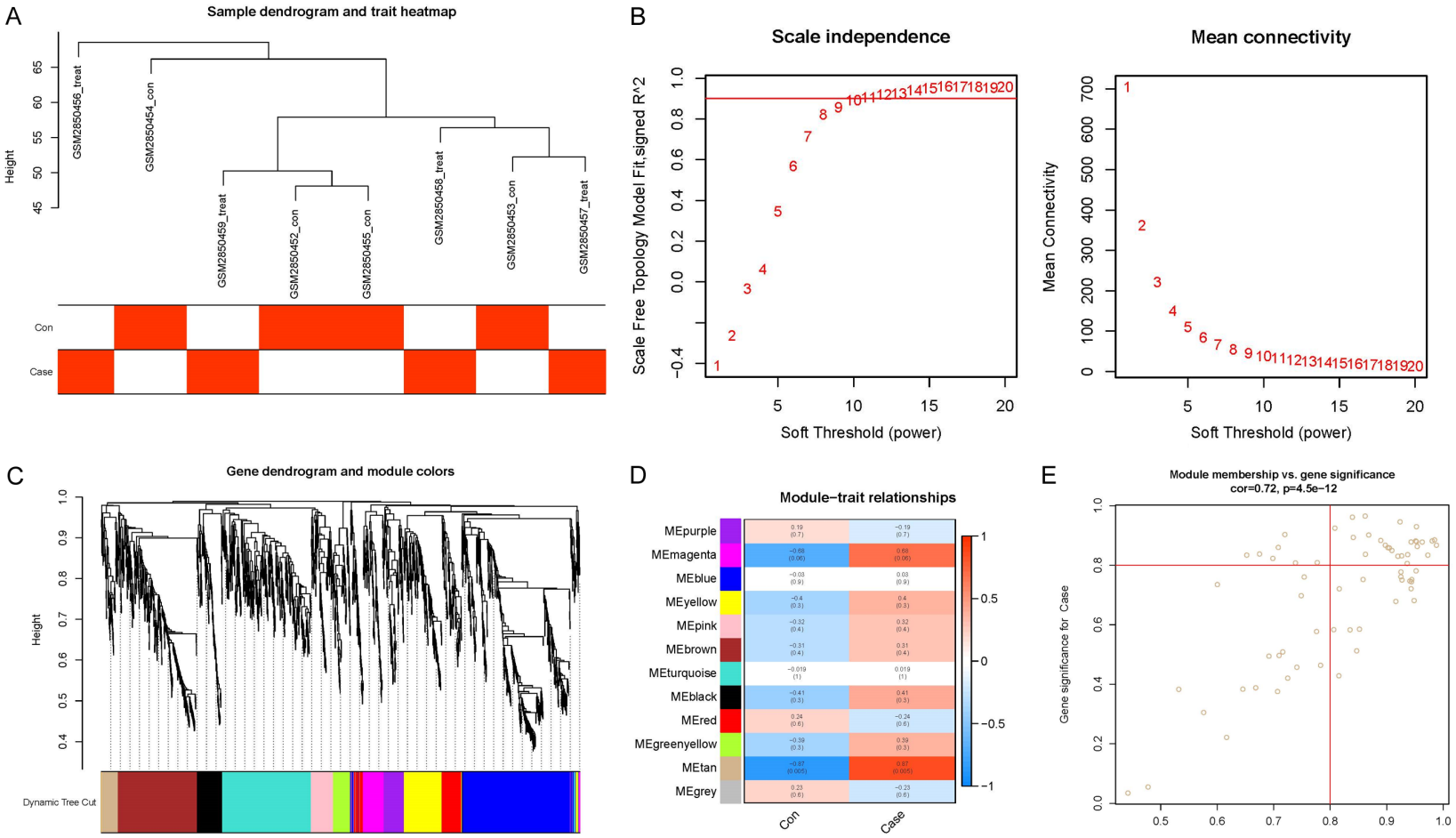

Figure 3. Identification of key module and genes via WGCNA. A. Clustering dendrogram of samples with trait heatmap. B. Analysis of network topology for various soft-thresholding powers. C. Clustering dendrogram of genes, with dissimilarity based on topological overlap, together with assigned module colors. D. Module-trait associations: each row corresponds to a module eigengene and each column to a trait. Each cell contains the corresponding correlation and *P* value. E. MM and GS scatter plots for the key module tan. The vertical line is |MM| = 0.8 and the horizontal line is |GS| = 0.8. The key genes of the module are in the box in the upper right corner. WGCNA: Weighted Gene Co-expression Network Analysis; GS: Gene Significance; MM: Module Membership.

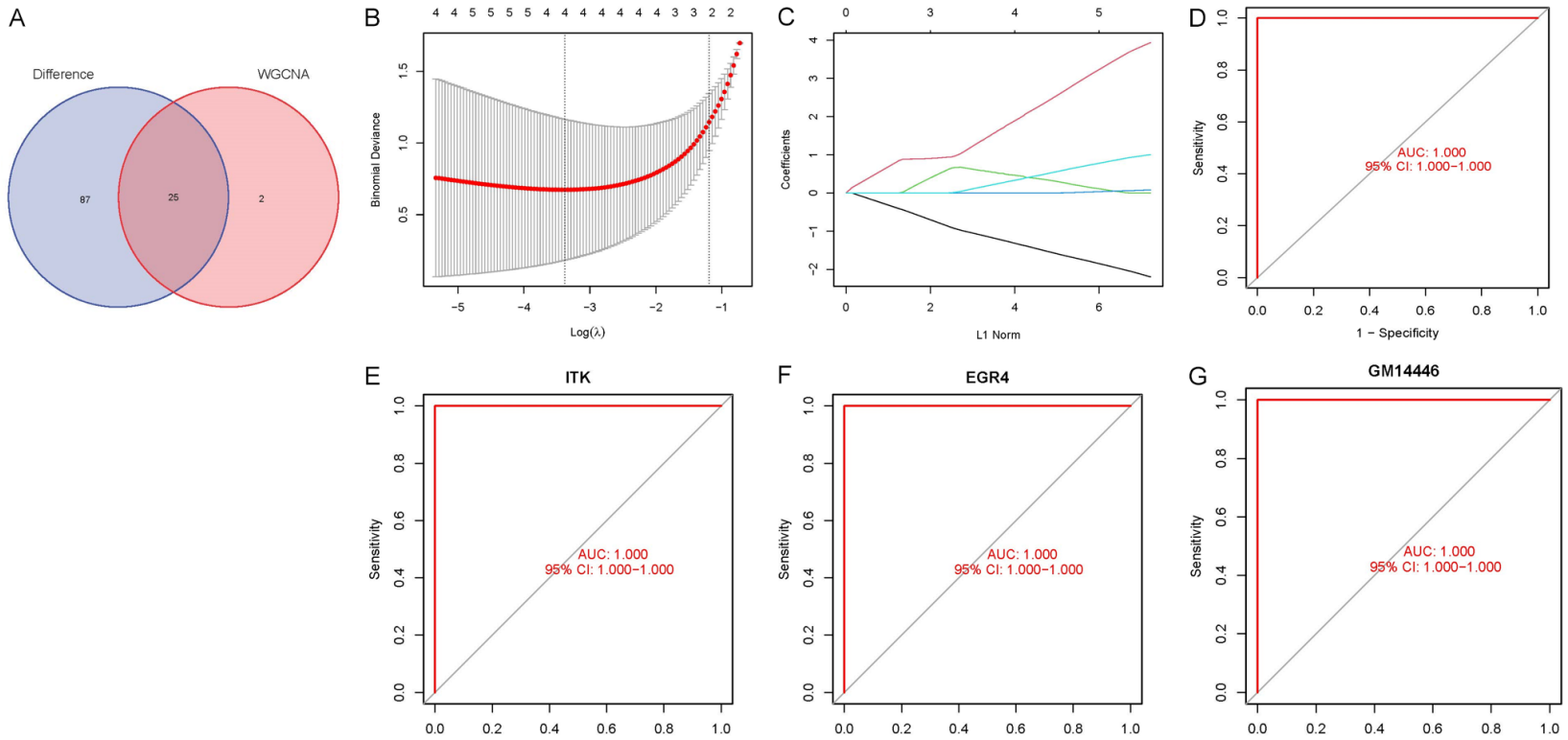

Figure 4. Screening of hub genes. A. Venn diagram of key module genes and DEGs. B. The most proper log λ value in the LASSO model. C. The log λ value of the DEGs related to propofol-induced neurotoxicity in the LASSO model. D-G. The areas under the ROC curve of 4 hub genes were all 1.0. DEDs: Differentially Expressed Genes; LASSO: Least Absolute Shrinkage and Selection Operator; ROC: Receiver Operating Characteristic.

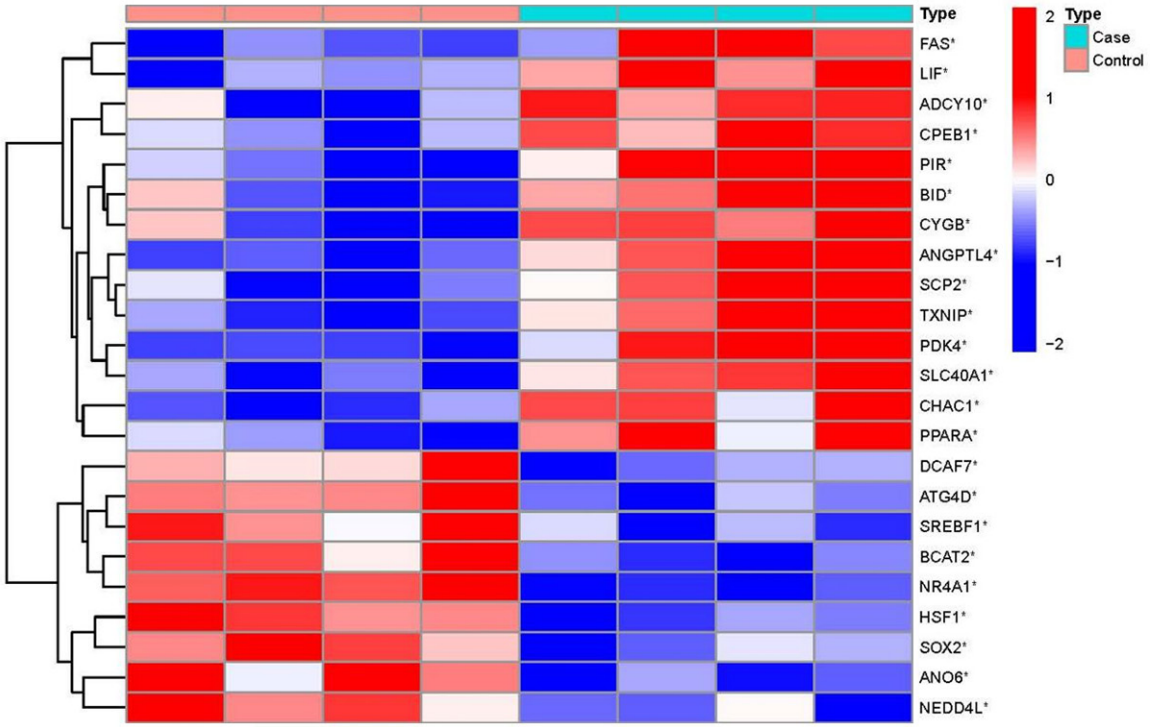

Figure 5. Heatmap of ferroptosis-related differentially expressed genes.

Hub gene ceRNA regulatory network

The ceRNA network showed that 44 lncRNAs and 13 miRNAs interacted with hub genes (*EGR4, HAO1, ITK* and *GM14446*). There were 74 edges in the ceRNA network (**Figure 6**).

Hub-gene-targeted drugs

We obtained 58 drugs that might be used to treat propofol-induced neurotoxicity via prediction using the CTD database (**Figure 7**).

Validation of hub gene and associated protein expression

The GSE106799 dataset revealed that the expressions of *HAO1, ITK* and *GM14446* were significantly higher in the case group than in the control group, but *EGR4* expression was lower in the case group (**Figure 8A-D**). Animal experiments demonstrated that propofol caused a significant increase in the mRNA levels of *HAO1, ITK* and *GM14446, and a* decreased level of *EGR4* in the brain tissue (**Figure 8E**). Western blotting suggested that the protein levels of HAO1, ITK, IL-6 and NF-κB were higher, while protein level of EGR4 was lower in the brain tissue from the case group than in that from the control group (**Figure 9A**, **9B**). We did not detect protein expression levels of *GM14446* because we did not obtain antibody to *GM14446*.

Discussion

Propofol, which is used for anesthesia induction and maintenance, is one of the most frequently used anesthetics. A growing number of preclinical data now suggest that propofol may induce neurotoxicity in pediatric surgery. Tu et al. found that propofol significantly inhibited the expression of brain-derived neurotropic factor (BDNF) in animal brains during the developmental stage, and BDNF plays an important role in the development and maturation of the neonatal nervous system [9, 10]. Some studies have suggested that anesthetic neurotoxicity may be one of the most important inducers of postoperative cognitive dysfunction that is characterized by memory and cognitive impairment [11]. Propofol may affect the process of ferroptosis in other diseases, and ferroptosis is known to play an important role in neurotoxicity and cognitive deficits [12-

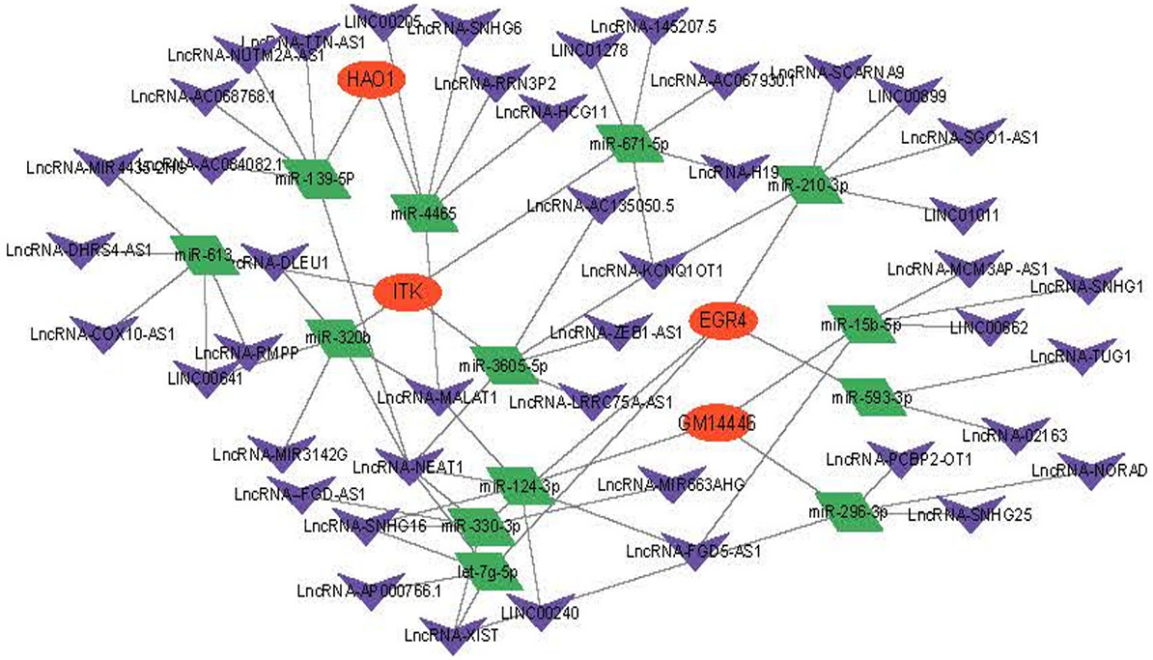

Figure 6. ceRNA network related to 4 hub genes. Orange ovals indicate hub genes, purple triangles indicate lncRNAs, and green diamonds indicate miRNAs.

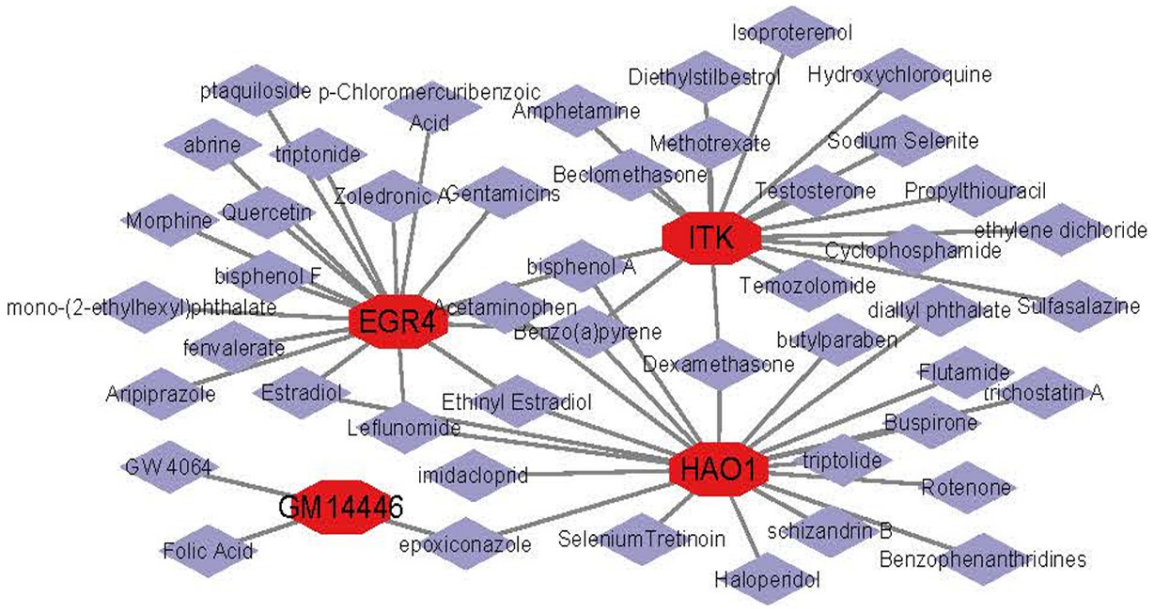

Figure 7. Drug-hub gene network. The red octagons represent hub genes, and purple diamonds represent drugs.

15]. In previous experiments we have learned that propofol can lead to neuronal apoptosis, neuroinflammation, neurodegeneration and synaptic alterations [16-18]. This study analyzed the specific mechanism of propofol-induced neurotoxicity from multiple perspectives by bioinformatics.

We identified 112 significant DEGs from the GSE106799 dataset and 25 key modular DEGs were obtained through WGCNA. By KEGG enrichment and GO functional analyses on all DEGs, we found that propofol-induced neurotoxicity involved 12 functional entries and 4 signaling pathways, such as somite rostral,

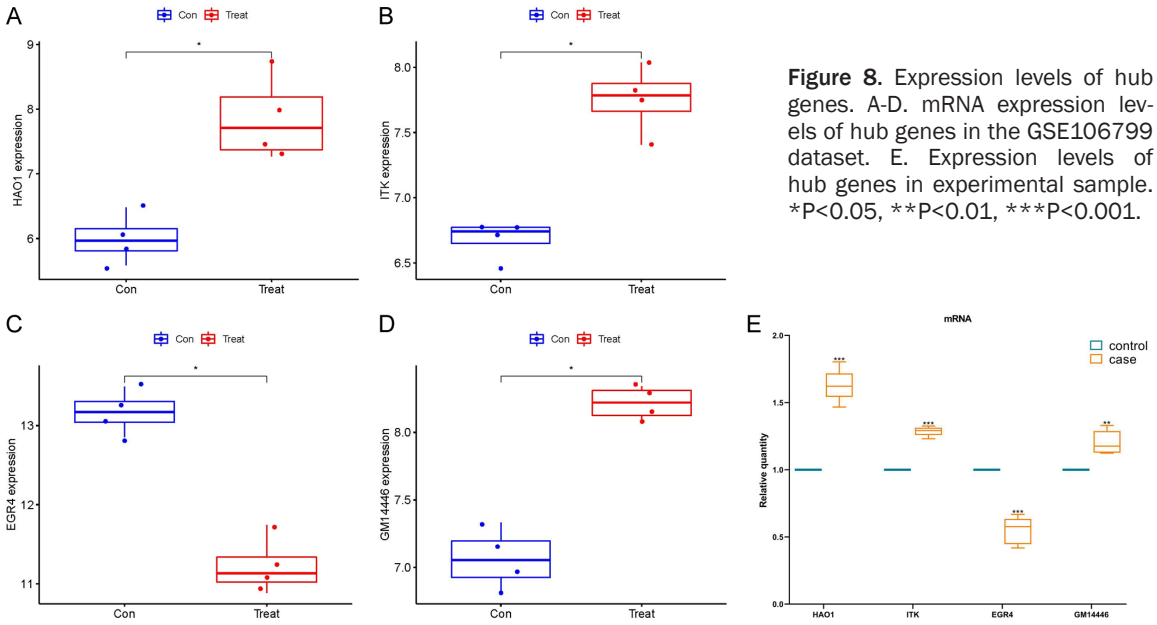

Figure 8. Expression levels of hub genes. A-D. mRNA expression levels of hub genes in the GSE106799 dataset. E. Expression levels of hub genes in experimental sample. *P<0.05, **P<0.01, ***P<0.001.

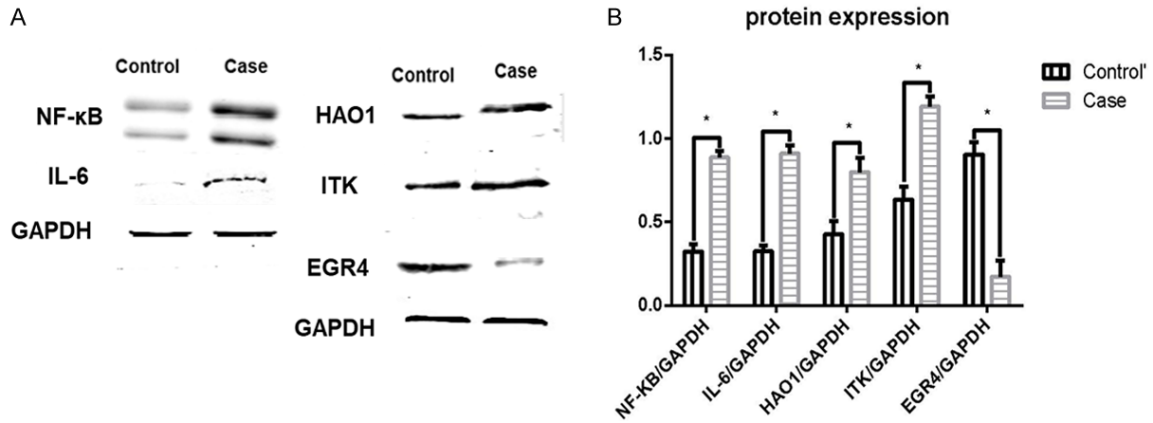

Figure 9. Western blotting validation of the expression levels of inflammatory factors and hub genes. A. Western blotting of NF-κB, IL-6, HAO1, ITK and EGR4. *P<0.05. B. Analysis of western bloting.

protein tyrosine, neuroactive ligand-receptor interaction and retinol metabolism. GSEA suggested that propofol-induced neurotoxicity was associated with processes such as activation of $CD8^+$ T cells, B cell maturation and transcription of Pam3CSK4. Enrichment analysis showed that propofol-induced neurotoxicity involved processes such as activation of immune cells and JAK/STAT and MAPK signaling pathways, nervous system development, vascular regeneration, and oxidative stress [19-23].

We obtained 4 hub genes (*EGR4, HAO1, ITK* and *GM14446*) of propofol-induced neurotoxicity after performing a LASSO regression analysis on 25 key modular DEGs. Western blotting suggested that propofol promoted the protein expressions of NF-κB, IL-6, HAO1 and ITK, while inhibited the protein expression of ERG4. qRT-PCR showed that the mRNA expressions of HAO1, ITK and GM14446 were higher in propofol-related samples than in the controls in both the GSE106799 dataset and experimental samples, but mRNA expression of EGR4 was contrary to that of HAO1, ITK and GM14446. HAO1 is a peroxisomal enzyme that can regulate the tricarboxylic acid cycle. Recalcati et al. found that HAO1 promoted the generation of H_2O_2 and was associated with iron metabolism

in oxidative stress [24, 25]. EGR4 is involved in the regulation of learning, synaptic plasticity and memory dysfunction, and is implicated in the pathogenesis of schizophrenia. EGR4 is required for the developmental upregulation of potassium-chloride ion cotransporter 2 (KCC2) gene expression. KCC2 plays a critical functional role in maintaining the balance of excitation-inhibition in the neonatal brain. EGR4 is also related to T cell activation and T helper (Th) cell differentiation [26-30]. ITK, which is essential for proximal T cell receptor signaling, negatively regulates the differentiation of $Foxp3^+$ regulatory T cells, which regulate the immune response through the production of transforming growth factor-β and IL-10 and depletion of IL-2. In contrast, ITK positively regulates the differentiation of Th17 cells, which are characterized as proinflammatory [31-33]. There is little information about GM14446, which may be related to antiviral function [34].

The roles of lncRNAs in neuronal development, maintenance and differentiation and neurodegenerative diseases are becoming increasingly evident. By predicting the miRNAs and lncRNAs associated with hub genes, a ceRNA network including 4 hub genes, 13 miRNAs, 44 lncRNAs and 74 edges was established. The above results lay a foundation for analyzing the pathophysiological mechanism of propofol-induced neurotoxicity. In addition, these RNAs have been shown to play a role in neuroprotection. For example, lncRNA XIST promotes the expression of IL-6 and TNF-α in neuroinflammation and angiogenesis via mediating miR-92a following ischemic stroke [35, 36]. lncRNA NEAT1 is associated with memory formation and the pathogenesis of various neurological diseases [37-39]. Finally, we found 58 potential drugs that may treat propofol-induced neurotoxicity. The above results indicate the basis of targeted therapy of hub genes.

There are still some shortcomings in our research. We did not verify whether knockdown of the hub genes could treat propofol-induced neurotoxicity in mice, because of lack of time and funding. The number of datasets about propofol-induced neurotoxicity is small.

In conclusion, we obtained 4 hub genes (EGR4, HAO1, ITK and GM14446) of propofol-induced neurotoxicity after analyzing the GSE106799 dataset via integrative bioinformatics. These potential targets may provide new directions for the prevention and treatment of propofol-induced neurotoxicity. Revealing the potential diagnostic and therapeutic value of these hub genes is our chief research objective in the future, which may ultimately aid the translation of these results into treatment.

Disclosure of conflict of interest

None.

Address correspondence to: Liang Cai, Department of Anesthesiology, The People's Hospital of Leshan, No. 238, Baita Street, Shizhong District, Leshan 614013, Sichuan, China. Tel: +86-0833-2119306; E-mail: m18780174951_1@163.com

References

[1] Ho AM, Fleming ML and Mizubuti GB. Anesthetic neurotoxicity and the developing brain. CMAJ 2017; 189: E1028-E1029.

[2] Lin EP, Soriano SG and Loepke AW. Anesthetic neurotoxicity. Anesthesiol Clin 2014; 32: 133-155.

[3] Bartkowska-Śniatkowska A, Rosada-Kurasińska J, Zielińska M and Bienert A. Do we really know the pharmacodynamics of anaesthetics used in newborns, infants and children? A review of the experimental and clinical data on neurodegeneration. Anaesthesiol Intensive Ther 2014; 46: 101-108.

[4] Xiu M, Luan H, Gu X, Liu C and Xu D. MicroRNA-17-5p protects against propofol anesthesia-induced neurotoxicity and autophagy impairment via targeting BCL2L11. Comput Math Methods Med 2022; 2022: 6018037.

[5] Liu F, Liu S, Patterson TA, Fogle C, Hanig JP, Wang C and Slikker W Jr. Protective effects of xenon on propofol-induced neurotoxicity in human neural stem cell-derived models. Mol Neurobiol 2020; 57: 200-207.

[6] Xiong M, Zhang L, Li J, Eloy J, Ye JH and Bekker A. Propofol-induced neurotoxicity in the fetal animal brain and developments in modifying these effects-an updated review of propofol fetal exposure in laboratory animal studies. Brain Sci 2016; 6: 11.

[7] Liu X, Ji J and Zhao GQ. General anesthesia affecting on developing brain: evidence from animal to clinical research. J Anesth 2020; 34: 765-772.

[8] Ma Z, Ma Y, Cao X, Zhang Y and Song T. Avenanthramide-C activates Nrf2/ARE pathway and inhibiting ferroptosis pathway to improve

cognitive dysfunction in aging rats. Neurochem Res 2022; [Epub ahead of print].
[9] Tu Y, Liang Y, Xiao Y, Lv J, Guan R, Xiao F, Xie Y and Xiao Q. Dexmedetomidine attenuates the neurotoxicity of propofol toward primary hippocampal neurons in vitro via Erk1/2/CREB/BDNF signaling pathways. Drug Des Devel Ther 2019; 13: 695-706.
[10] Camuso S, La Rosa P, Fiorenza MT and Canterini S. Pleiotropic effects of BDNF on the cerebellum and hippocampus: implications for neurodevelopmental disorders. Neurobiol Dis 2022; 163: 105606.
[11] Li GF, Li ZB, Zhuang SJ and Li GC. Inhibition of microRNA-34a protects against propofol anesthesia-induced neurotoxicity and cognitive dysfunction via the MAPK/ERK signaling pathway. Neurosci Lett 2018; 675: 152-159.
[12] Liu YP, Qiu ZZ, Li XH and Li EY. Propofol induces ferroptosis and inhibits malignant phenotypes of gastric cancer cells by regulating miR-125b-5p/STAT3 axis. World J Gastrointest Oncol 2021; 13: 2114-2128.
[13] Li S, Lei Z, Yang X, Zhao M, Hou Y, Wang D, Tang S, Li J and Yu J. Propofol protects myocardium from ischemia/reperfusion injury by inhibiting ferroptosis through the AKT/p53 signaling pathway. Front Pharmacol 2022; 13: 841410.
[14] Wu J, Yang JJ, Cao Y, Li H, Zhao H, Yang S and Li K. Iron overload contributes to general anaesthesia-induced neurotoxicity and cognitive deficits. J Neuroinflammation 2020; 17: 110.
[15] Zhang P, Chen Y, Zhang S and Chen G. Mitochondria-related ferroptosis drives cognitive deficits in neonatal mice following sevoflurane administration. Front Med (Lausanne) 2022; 9: 887062.
[16] Liang C, Du F, Cang J and Xue Z. Pink1 attenuates propofol-induced apoptosis and oxidative stress in developing neurons. J Anesth 2018; 32: 62-69.
[17] Milanovic D, Pesic V, Loncarevic-Vasiljkovic N, Pavkovic Z, Popic J, Kanazir S, Jevtovic-Todorovic V and Ruzdijic S. The Fas ligand/Fas death receptor pathways contribute to propofol-induced apoptosis and neuroinflammation in the brain of neonatal rats. Neurotox Res 2016; 30: 434-452.
[18] Yan Y, Logan S, Liu X, Chen B, Jiang C, Arzua T, Ramchandran R, Liu QS and Bai X. Integrated excitatory/inhibitory imbalance and transcriptomic analysis reveals the association between dysregulated synaptic genes and anesthetic-induced cognitive dysfunction. Cells 2022; 11: 2497.
[19] Al-Rashed F, Kochumon S, Usmani S, Sindhu S and Ahmad R. Pam3CSK4 induces MMP-9 expression in human monocytic THP-1 cells. Cell Physiol Biochem 2017; 41: 1993-2003.
[20] Yin T, Yang L and Yang YC. Tyrosine phosphorylation and activation of JAK family tyrosine kinases by interleukin-9 in MO7E cells. Blood 1995; 85: 3101-3106.
[21] Wang F, Liu W, Ma J, Yu M, Jin Y and Dai J. Prenatal and neonatal exposure to perfluorooctane sulfonic acid results in changes in miRNA expression profiles and synapse associated proteins in developing rat brains. Environ Sci Technol 2012; 46: 6822-6829.
[22] Kazemi M, Shokri S, Ganjkhani M, Ali R and Iraj JA. Modulation of axonal sprouting along rostro-caudal axis of dorsal hippocampus and no neuronal survival in parahippocampal cortices by long-term post-lesion melatonin administration in lithium-pilocarpine model of temporal lobe epilepsy. Anat Cell Biol 2016; 49: 21-33.
[23] Yang T, Chen L, Dai Y, Jia F, Hao Y, Li L, Zhang J, Wu L, Ke X, Yi M, Hong Q, Chen J, Fang S, Wang Y, Wang Q, Jin C, Chen J and Li T. Vitamin a status is more commonly associated with symptoms and neurodevelopment in boys with autism spectrum disorders-a multicenter study in China. Front Nutr 2022; 9: 851980.
[24] Recalcati S, Tacchini L, Alberghini A, Conte D and Cairo G. Oxidative stress-mediated downregulation of rat hydroxyacid oxidase 1, a liver-specific peroxisomal enzyme. Hepatology 2003; 38: 1159-1166.
[25] Kimura A, Hirayama A, Matsumoto T, Sato Y, Kobayashi T, Ikeda S, Maruyama M, Kaneko M, Shigeta M, Ito E, Soma T, Miyamoto K, Soga T, Tomita M, Oya A, Matsumoto M, Nakamura M, Kanaji A and Miyamoto T. Hao1 is not a pathogenic factor for ectopic ossifications but functions to regulate the TCA cycle in vivo. Metabolites 2022; 12: 82.
[26] Cheng MC, Chuang YA, Lu CL, Chen YJ, Luu SU, Li JM, Hsu SH and Chen CH. Genetic and functional analyses of early growth response (EGR) family genes in schizophrenia. Prog Neuropsychopharmacol Biol Psychiatry 2012; 39: 149-155.
[27] Raol YH, Joksimovic SM, Sampath D, Matter BA, Lam PM, Kompella UB, Todorovic SM and González MI. The role of KCC2 in hyperexcitability of the neonatal brain. Neurosci Lett 2020; 738: 135324.
[28] Djankpa FT, Akinola OB and Juliano SL. Distribution and cellular localization of KCC2 in the ferret neocortex. Dev Neurosci 2018; 40: 39-53.
[29] Mookerjee-Basu J, Hooper R, Gross S, Schultz B, Go CK, Samakai E, Ladner J, Nicolas E, Tian Y, Zhou B, Zaidi MR, Tourtellotte W, He S, Zhang Y, Kappes DJ and Soboloff J. Suppression of Ca(2+) signals by EGR4 controls Th1 differentiation and anti-cancer immunity in vivo. EMBO Rep 2020; 21: e48904.

[30] Goutierre M, Al Awabdh S, Donneger F, François E, Gomez-Dominguez D, Irinopoulou T, Menendez de la Prida L and Poncer JC. KCC2 regulates neuronal excitability and hippocampal activity via interaction with task-3 channels. Cell Rep 2019; 28: 91-103, e7.
[31] Elmore JP, McGee MC, Nidetz NF, Anannya O, Huang W and August A. Tuning T helper cell differentiation by ITK. Biochem Soc Trans 2020; 48: 179-185.
[32] Weeks S, Harris R and Karimi M. Targeting ITK signaling for T cell-mediated diseases. iScience 2021; 24: 102842.
[33] Lechner KS, Neurath MF and Weigmann B. Role of the IL-2 inducible tyrosine kinase ITK and its inhibitors in disease pathogenesis. J Mol Med (Berl) 2020; 98: 1385-1395.
[34] Mears HV and Sweeney TR. Mouse Ifit1b is a cap1-RNA-binding protein that inhibits mouse coronavirus translation and is regulated by complexing with Ifit1c. J Biol Chem 2020; 295: 17781-17801.
[35] Li WX, Qi F, Liu JQ, Li GH, Dai SX, Zhang T, Cheng F, Liu D and Zheng SG. Different impairment of immune and inflammation functions in short and long-term after ischemic stroke. Am J Transl Res 2017; 9: 736-745.
[36] Zhang M, Yang JK and Ma J. Regulation of the long noncoding RNA XIST on the inflammatory polarization of microglia in cerebral infarction. Exp Ther Med 2021; 22: 924.
[37] Butler AA, Johnston DR, Kaur S and Lubin FD. Long noncoding RNA NEAT1 mediates neuronal histone methylation and age-related memory impairment. Sci Signal 2019; 12: eaaw9277.
[38] Wei X, Xu S and Chen L. LncRNA Neat1/miR-298-5p/Srpk1 contributes to sevoflurane-induced neurotoxicity. Neurochem Res 2021; 46: 3356-3364.
[39] Zhou ZW, Ren X, Zheng LJ, Li AP and Zhou WS. LncRNA NEAT1 ameliorate ischemic stroke via promoting Mfn2 expression through binding to Nova and activates Sirt3. Metab Brain Dis 2022; 37: 653-664.